The nuclear physics of neutron stars

J. Piekarewicz
Department of Physics, Florida State University,
Tallahassee, FL 32306.

Recibido el 13 de abril de 2008; aceptado el 23 de junio de 2008

A remarkable fact about spherically-symmetric neutron stars in hydrostatic equilibrium — the so-called Schwarzschild stars — is that the only physics that they are sensitive to is the equation of state of neutron-rich matter. As such, neutron stars provide a myriad of observables that may be used to constrain poorly known aspects of the nuclear interaction under extreme conditions of density. After discussing many of the fascinating phases encountered in neutron stars, I will address how powerful theoretical, experimental, and observational constraints may be used to place stringent limits on the equation of state of neutron-rich matter.

Keywords: Nuclear matter; neutron stars; effective interactions.

Un hecho sorprendente acerca de las estrellas de neutrones con simetria esferica y en equilibrio hydrostatico — las llamadas estrellas de Schwarzschild — es que su dinámica solo depende de la ecuación de estado de materia nuclear asimétrica. Por lo tanto, las estrellas de neutrones proporcionan una gran diversidad de observables que pueden ser utilizadas para determinar las interacciones nucleares bajo condiciones extremas de densidad. Despues de introducir varias fases presentes en las estrellas de neutrones, discutire como usar argumentos teóricos, experimentales y observacionales para limitar la ecuacion de estado de materia nuclear asimétrica.

Descriptores: Materia nuclear; estrellas de neutrones; interacciones efectivas.

PACS: 21.65.+f; 26.60.+c; 21.30.Fe

1. Introduction

A neutron star is a gold mine for the study of the phase diagram of cold baryonic matter. While the most common perception of a neutron star is that of a uniform assembly of neutrons packed to densities that may exceed that of normal nuclei by up to an order of magnitude, the reality is far different and significantly more interesting. Indeed, the mere fact that hydrostatic equilibrium must be maintained throughout the neutron star, demands a *negative* pressure gradient at each point in the star; otherwise the star would collapse under its own weight. This model-independent fact yields nuclear densities — at least for most realistic equations of states — that span over 11 orders of magnitude; from 10^4 to 10^{15}g/cm^3. Recall that in this units nuclear-matter saturation density equals $\rho_0 = 2.48 \times 10^{14}$g/cm^3. What novels phases of baryonic matter emerge under these conditions is both fascinating and unknown. Moreover, most of the exotic phases predicted to exist in neutron stars can not be realized under normal laboratory conditions. Whereas most of these phases have a fleeting existence here on Earth, they become stable in neutron stars as a consequence of the presence of enormous gravitational fields.

To establish the fundamental role played by the equation of state on the structure of spherically-symmetric neutron stars in hydrostatic equilibrium, we start with the Tolman-Oppenheimer-Volkoff (TOV) equations — the extension of Newton's laws to the domain of general relativity. The TOV equations may be expressed as a coupled set of first-order differential equations of the following form:

$$\frac{dP}{dr} = -G\,\frac{\mathcal{E}(r)M(r)}{r^2}\left[1+\frac{P(r)}{\mathcal{E}(r)}\right] \times \left[1+\frac{4\pi r^3 P(r)}{M(r)}\right]\left[1-\frac{2GM(r)}{r}\right]^{-1}, \quad (1)$$

$$\frac{dM}{dr} = 4\pi r^2 \mathcal{E}(r)\,, \quad (2)$$

where G is Newton's gravitational constant, while $P(r)$, $\mathcal{E}(r)$, and $M(r)$ represent the pressure, energy density, and enclosed-mass profiles of the star, respectively. Note that the last three terms (enclosed in square brackets) in Eq. (1) have a general-relativistic origin. Remarkably, the only input that neutron stars are sensitive to is the equation of state of neutron-rich matter. Indeed, changes in pressure and enclosed mass as a function of radius (left-hand side of the equations) depend not only on the values of these quantities at r, but also on the "unknown" energy density $\mathcal{E}(r)$ of the system. Thus, no solution of the TOV equations is possible until an equation of state (*i.e.*, a P *vs* $\mathcal{E}$ relation) is supplied.

In this manuscript we discuss the various fascinating phases of baryonic matter that are predicted to exist in neutron stars, but inaccessible under normal laboratory conditions. After briefly discussion the theoretical models used in this contribution, we focus on recent theoretical, experimental, and observational constrains that place stringent limits on the equation of state of neutron-rich matter.

2. Anatomy of a neutron star

Neutron stars contain a non-uniform crust above a uniform liquid mantle. See Fig. 1 for what is believed to be an accurate rendition of the structure of a neutron star.

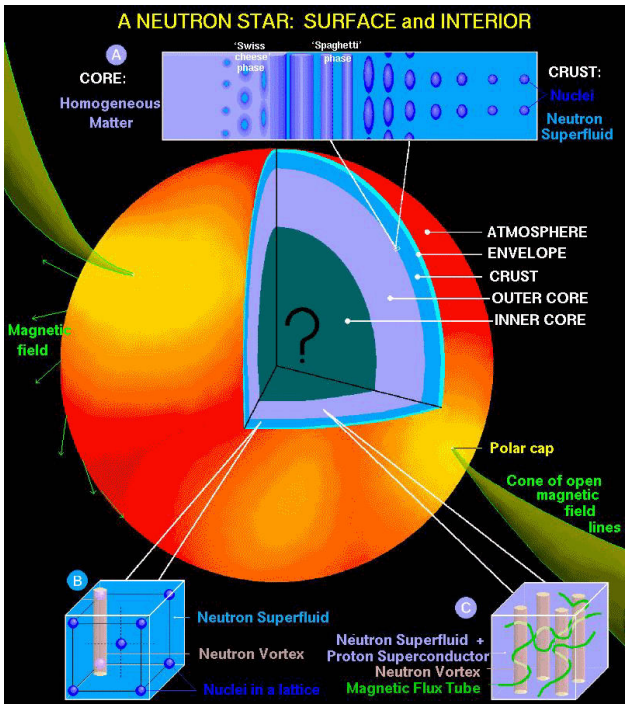

FIGURE 1. A rendition of the structure and phases of a neutron star (courtesy of Dany Page).

2.1. The outer crust

The outer crust is understood as the region of the star spanning about 7 orders of magnitude in density; from about $10^4 \mathrm{g/cm}^3$ to $4 \times 10^{11} \mathrm{g/cm}^3$ [1]. At these densities, the electrons — which are an essential component of the star in order to maintain charge neutrality — have been pressure ionized and move freely throughout the crust. Moreover, at these "low" densities, ^{56}Fe nuclei arrange themselves in a crystalline lattice in order to minimize their overall Coulomb repulsion. This is the structure of the outermost layer of the crust. However, as the density increases (and one moves away from the surface of the star) ^{56}Fe is no longer the most energetically favorable nucleus. This is because the electronic contribution to the energy increases faster with density than the nuclear contribution. As a result, it becomes energetically advantageous for the energetic electrons to capture on the protons and for the excess energy to be carried away by neutrinos. The resulting nuclear lattice is now made of nuclei having a neutron excess larger than that of ^{56}Fe. As the density continues to increase, the nuclear system evolves into a Coulomb lattice of progressively more neutron-rich nuclei until a *"critical"* density of about $4 \times 10^{11} \mathrm{g/cm}^3$ is reached. At this point the nuclei are unable to hold any more neutrons; the neutron drip line has been reached.

2.2. The inner crust

The inner crust of the neutron star comprises the region from neutron-drip density up to the density at which uniformity in the system is restored (approximately $1/3$ to $1/2$ of normal nuclear matter saturation density). At these densities the system exhibits rich and complex structures that emerge from a dynamical competition between short-range nuclear attraction and long-range Coulomb repulsion. At the lower densities present in the *outer core*, these length scales are well separated and the system organizes itself into a crystalline lattice of neutron-rich nuclei. In contrast, at a much higher density of the order of half of nuclear-matter saturation density, uniformity in the system is restored and the system behaves as a uniform Fermi liquid. Yet the transition region from the highly-ordered crystal to the uniform liquid mantle is complex and not well understood. Length scales that were well separated in both the crystalline and uniform phases are now comparable, giving rise to a universal phenomenon known as *"Coulomb frustration"*. It has been speculated that the transition to the uniform phase *must* go through a series of changes in the dimensionality and topology of these complex structures, colloquially known as *"nuclear pasta"* [2,3]. In Fig. 2 a snapshot obtained from Monte-Carlo/Molecular-Dynamics simulations of a nuclear system at densities relevant to the inner crust are displayed [4,5]. The figure displays how the system organizes itself into neutron-rich clusters (*i.e.,* "nuclei") of complex topologies that are surrounded by a vapor of (perhaps superfluid) neutrons. Such complex pasta structures may have a significant impact on various transport properties, such as neutrino and electron propagation.

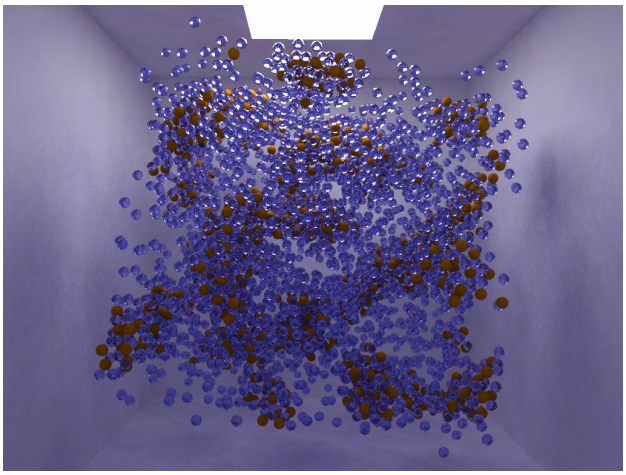

FIGURE 2. (color online) A snapshot of a Monte Carlo simulation for a configuration of 4,000 nucleons at a baryon density of $n = 0.025$ fm^{-3} (a sixth of normal nuclear matter saturation density), a proton fraction of $Y_p = Z/A = 0.2$, and a temperature of $T = 1$ MeV.

2.3. The stellar core

As the density continues to increase, the neutron-rich nuclei will "melt" and uniformity in the system will be restored. At these densities (of the order of 1/3-to-1/2 of normal nuclear-matter saturation density) the naive perception of a neutron star, namely, a uniform assembly of closely-packed neutrons will be realized, albeit for the presence of a small percentage (of the order of 10%) of protons and electrons required

to maintain chemical equilibrium and charge neutrality. Although the non-uniform crust displays fascinating and intriguing dynamics, its structural impact on the star is rather modest. Indeed, the crust accounts for about 10% of the radius of the neutron star and for only a few percent of its mass. Most of the mass of the neutron star is contained in its uniform core. Yet the highest density attained in the core depends critically on the equation of state of neutron-rich matter which at those high densities is poorly constrained. The cleanest constraint on the equation of state at high-density will emerge as we answer one of the central questions in nuclear astrophysics: *what is the maximum mass of a neutron star?* Or equivalently, *what is the minimum mass of a black hole?* Note that if the equation of state is "soft", very high densities may be reached in the stellar core. At such high densities new states of matter may develop as the quarks within the hadrons become deconfined. Such an exciting possibility will not be considered further in this manuscript.

3. Constraints on the equation of state

Before addressing the role that recent observables play in constraining various theoretical description of the equation of state, we introduce the relativistic mean-field models that are used to compute these observables.

Relativistic mean-field descriptions of the ground-state properties of medium to heavy nuclei have enjoyed enormous success. These highly economical descriptions encode a great amount of physics in a handful of model parameters that are calibrated to a few ground-state properties of a representative set of medium to heavy nuclei. An example of such a successful paradigm is the relativistic NL3 parameter set of Lalazissis, Ring, and collaborators [6,7].

The Lagrangian density employed in this work is rooted on the seminal work of Walecka, Serot, and their many collaborators (see Refs. 8 to 10 and references therein). Since first published by Walecka more than three decades ago [8], several refinements have been implemented to improve the quantitative standing of the model. In the present work we employ an interacting Lagrangian density of the following form[11-13]:

$$\begin{aligned}\mathscr{L}_{\rm int} = \bar{\psi}\left[g_{\rm s}\phi - \left(g_{\rm v}V_\mu + \frac{g_\rho}{2}\tau\cdot\mathbf{b}_\mu + \frac{e}{2}(1+\tau_3)A_\mu\right)\gamma^\mu\right]\psi \\ - \frac{\kappa}{3!}(g_{\rm s}\phi)^3 - \frac{\lambda}{4!}(g_{\rm s}\phi)^4 + \frac{\zeta}{4!}\left(g_{\rm v}^2V_\mu V^\mu\right)^2 \\ + \Lambda_{\rm v}\left(g_\rho^2\,\mathbf{b}_\mu\cdot\mathbf{b}^\mu\right)\left(g_{\rm v}^2V_\mu V^\mu\right). \qquad (3)\end{aligned}$$

The original Lagrangian density of Walecka consisted of an isodoublet nucleon field (ψ) together with neutral scalar (ϕ) and vector (V^μ) fields coupled to the scalar density ($\bar{\psi}\psi$) and conserved nucleon current ($\bar{\psi}\gamma^\mu\psi$), respectively [8]. In spite of its simplicity (indeed, the model contains only two dimensionless coupling constants), symmetric nuclear matter saturates even when the model was solved at the mean-field level [8]. By adding additional contributions from a single isovector meson (b^μ) and the photon (A^μ), Horowitz and Serot [14] obtained results for the ground-state properties of finite nuclei that rivaled some of the most sophisticated non-relativistic calculations of the time. However, whereas the two dimensionless parameters in the original Walecka model could be adjusted to reproduce the nuclear saturation point, the incompressibility coefficient (now a prediction of the model) was too large ($K \gtrsim 500$ MeV) as compared with existing data on breathing-mode energies [15]. To overcome this problem, Boguta and Bodmer introduced cubic (κ) and quartic (λ) scalar meson self-interactions that accounted for a significant softening of the equation of state ($K = 150 \pm 50$ MeV) [16]. Two parameters of the Lagrangian density of Eq. (3) remain to be discussed, namely, ζ and $\Lambda_{\rm v}$. Both of these parameters are set to zero in the enormously successful NL3 model, suggesting that the experimental data used in the calibration procedure is insensitive to the physics encoded in these parameters. Indeed, Müller and Serot found possible to build models with different values of ζ that reproduce the same observed properties at normal nuclear densities, but which yield maximum neutron star masses that differ by almost one solar mass [12]. This result indicates that observations of massive neutron stars — rather than laboratory experiments — may provide the only meaningful constraint on the high-density component of the equation of state. Finally, the isoscalar-isovector coupling constant $\Lambda_{\rm v}$ was added in Ref. 13 to modify the density dependence of the symmetry energy. It was found that models with different values of $\Lambda_{\rm v}$ reproduce the same exact properties of symmetric nuclear matter, but yield vastly different values for the neutron skin thickness of heavy nuclei and for the radii of neutron stars [17]. The Parity Radius Experiment (PREx) at the Jefferson Laboratory promises to measure the skin thickness of ^{208}Pb accurately and model independently via parity-violating electron scattering [18,19]. PREx will provide a unique experimental constraint on the density dependence of the symmetry energy due its strong correlation to the neutron skin of heavy nuclei [20].

3.1. Theoretical constraints

One of the most stringent constraints on the equation of state of low density neutron-rich matter emerges from theoretical considerations, namely, from the universality of dilute Fermi gases with an "infinite" scattering length (a). In this limit the only energy scale in the problem is the Fermi energy ($\varepsilon_{\rm F}$), so the energy per particle is constrained to be that of the free Fermi gas up to a dimensionless *universal constant* (ξ) that is independent of the details of the two-body interaction [21]. That is,

$$\frac{E}{N} = \xi\frac{3}{5}\varepsilon_{\rm F}\ . \qquad (4)$$

To date, the best theoretical estimates place the value of the universal constant around $\xi \approx 0.4$ [21-24].

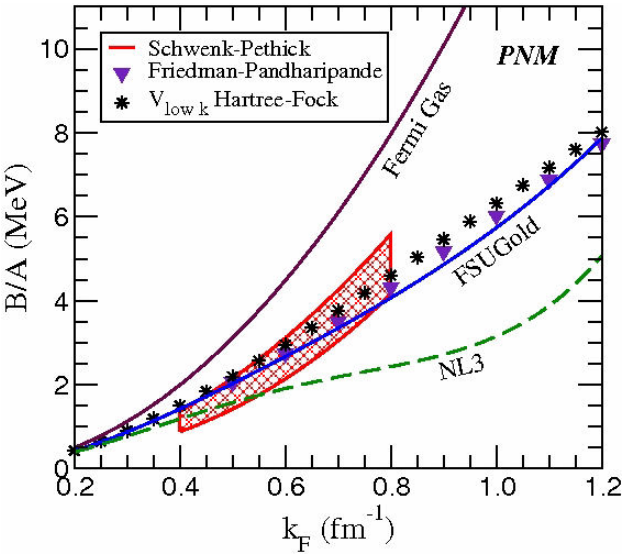

FIGURE 3. (color online) Equation of state of pure neutron matter as a function of the Fermi momentum. Predictions are shown for the accurately calibrated NL3 [6,7] (green line) and FSUGold [11] (blue line) parameter sets. Shown also are various microscopic descriptions — including a *model-independent* result based on the physics of resonant Fermi gases by Schwenk and Pethick [25] (red region).

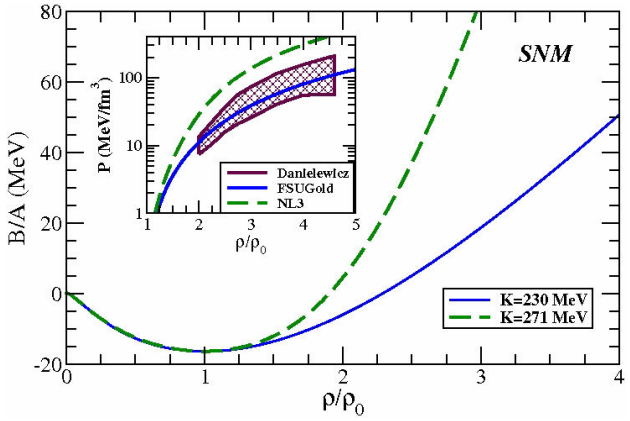

FIGURE 4. (color online) Binding energy per nucleon as a function of baryon density (expressed in units of the saturation density $\rho_0 = 0.148\ \mathrm{fm}^{-3}$) for symmetric nuclear matter. Theoretical predictions are shown for the NL3 [6,7] (green line) and FSUGold [11] (blue line) models. Shown in the inset is a comparison between the equation of state extracted from energetic nuclear collisions [27] and the predictions of these two models.

Although the neutron-neutron scattering length is large indeed ($a_{\rm nn} = -18.5$ fm), pure neutron matter deviates from unitarity due to a non-negligible value of the effective range of the neutron-neutron interaction ($r_{\rm e} = +2.7$ fm). Thus, corrections to the low-density equation of state of pure neutron matter must be computed for $k_{\rm F} \sim r_{\rm e}^{-1} \simeq 0.4\ \mathrm{fm}^{-1}$. Such corrections have been recently computed by Schwenk and Pethick [25], with their results displayed as the red hatched region in Fig 3. Also shown are the predictions of two microscopic models based on realistic two-body interactions, one of them being the venerated equation of state of Friedman and Pandharipande [26]. Finally, the predictions of NL3 and FSUGold are also shown. It is gratifying that the softening of the symmetry energy of FSUGold — caused by incorporating constraints from breathing-mode energies [11] — appears consistent with the physics of resonant Fermi gases. Such a powerful universal constraint should be routinely and explicitly incorporated into future determinations of density functionals. Indeed, such a constrain appears to rule out many of the models displayed in Fig. 2 of Ref. 20.

3.2. Experimental constraints

Energetic nuclear collisions may be used to constrain the high-density behavior of nucleonic matter. To illustrate this point we display in Fig. 4 the binding energy per nucleon of *symmetric* nuclear matter as a function of the baryon density as predicted by both the NL3 and FSUGold models. Note that both models reproduce the equilibrium properties of symmetric nuclear matter and display the same *quantitative* behavior at densities below the saturation point. Yet their high-density predictions are significantly different. This emerges from a combination of two factors. First, FSUGold predicts an incompressibility coefficient K considerably lower than NL3, namely, 230 MeV *vs* 271 MeV. Second, and more importantly, FSUGold includes an omega-meson self-energy coupling [labeled by ζ in Eq. (3)] that is responsible for a significant softening at high density. We now compare the predictions of these two models against results obtained from energetic nuclear collisions that can compress baryonic matter to densities as high as those predicted to exist in the core of neutron stars. The inset in Fig. 4 provides us with such a comparison. By analyzing the manner in which matter flows after the collision of two energetic gold nuclei, the equation of state of *symmetric* nuclear matter was extracted up to densities of 4-to-5 times saturation density [27]. Figure 4 seems to rule out overly stiff equations of state (such as NL3). And while it is gratifying that FSUGold is consistent with this analysis, one must stress that the connection between energetic nuclear collisions and the equation of state of cold nuclear matter is model dependent.

3.3. Observational constraints

A recent observation that seems to suggest a hard equation of state is that of the low-mass X-ray binary EXO 0748-676. Note that such a binary system consists of a neutron star accreting mass from a normal (non-compact) companion. The first constraint on the equation of state from such an object came from the detection of gravitationally redshifted absorption lines in Oxygen and Iron by Cottam and collaborators [28]. By measuring a gravitational redshift of $z = 0.35$, the mass-to-radius *ratio* of the neutron star gets fixed at $M/R \simeq 0.15$ (with M expressed in solar masses and R in kilometers). By incorporating additional constraints arising from Eddington and thermal fluxes, a recent analysis by Özel seems to place *simultaneous* limits on the mass and

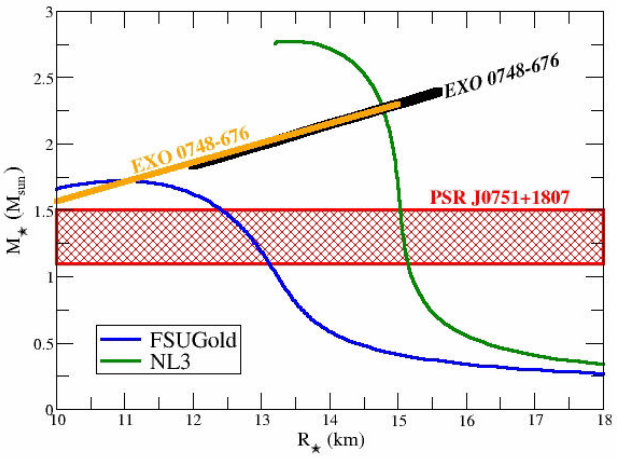

FIGURE 5. (color online) Constraints on the mass-vs-radius relationship of neutron stars. Displayed in red is the *recently revised* region allowed by the analysis of Nice and collaborators [31]. The black and orange solid lines result from the analyzes of EXO 0748-676 by Özel [29], and Villarreal and Strohmayer [30], respectively. Also shown are the theoretical predictions from the NL3 [6,7] (green line) and FSUGold [11] (blue line) models.

radius of the neutron star in EXO 0748-676. That is, $M \geq 2.10 \pm 0.28\ M_\odot$ and $R \geq 13.8 \pm 1.80$ km [29]. These limits are indicated by the black solid line in Fig. 5. An earlier determination of the spin frequency of the same neutron star by Villarreal and Strohmayer [30], when combined with the rotational broadening of surface spectral lines, yields an independent determination of the stellar radius of $R \approx 11.5^{+3.5}_{-2.5}$ km. This estimate, when combined with the gravitational redshift, yields the orange line in Fig.5. Finally, *mass-vs-radius* predictions from the NL3 and FSUGold models are displayed in Fig. 5. The results clearly indicate the significantly harder character of the equation of state predicted by NL3 relative to FSUGold. This, even when both models predict practically identical properties for existent ground-state observables of finite nuclei.

A critical observation that would have impacted significantly on the high-density component of equation of state is the one by Nice and collaborators at the Arecibo radio telescope [31]. Such (initial) observation of a neutron-star–white-dwarf binary system suggested a neutron-star mass of $M(\text{PSR J0751}+1807) = 2.1 \pm 0.2\ M_\odot$. This was the largest neutron-star mass ever reported and promised, provided that the errors could be tighten further, to practically pin down the high-density component of the equation of state. However, at a very recent conference celebrating the 40th anniversary of the discovery of pulsars in Montreal, Nice reported a significantly reduced value for the mass of PSR J0751+1807, namely, $M(\text{PSR J0751}+1807) \approx 1.3 \pm 0.2\ M_\odot$. This revised result is denoted by the red hatched region in Fig. 5 and no longer invalidates any of the theoretical models under consideration.

4. Conclusions

Neutron stars are unique laboratory for the study of cold baryonic matter over an enormous range of densities. After an introduction to the "anatomy" of a neutron star, I relied on recent theoretical, experimental, and observational constraints to elucidate important features of the equation of state of neutron-rich matter. As mentioned in the Introduction, the only physics that spherically-symmetric neutron stars in hydrostatic equilibrium are sensitive to is the equation of state of neutron-rich matter [see Eqs. (1 and 2)]. This makes neutron stars gold mines for the study of baryonic matter. The various constraints utilized in this contribution emerged from the universal behavior of dilute Fermi gases with large scattering lengths [25], heavy-ion experiments that probe the high-density domain of the equation of state [27], and astronomical observations that place limits on masses and radii of neutron stars [29,31]. On the basis of these comparisons, it was concluded that FSUGold meets all the challenges, even when no attempt was ever made to incorporate these constraints into the calibration procedure. The promise of new terrestrial laboratories (such as *Facilities for Rare Ion Beams*) together with improved observations with existent and future missions (such as *Constellation X*) offers the greatest hope for determining the equation of state of cold baryonic matter in the near future.

Acknowledgments

The author is grateful to the organizers of the *XXXI Symposium on Nuclear Physics* for their kind invitation and hospitality. The author also wishes to acknowledge his many collaborators that were involved in this work — especially Prof. C.J. Horowitz. This work was supported in part by United States Department of Energy under grant DE-FD05-92ER40750.

1. G. Baym, C. Pethick, and P. Sutherland, *Astrophys. J.* **170**, (1971) 299.
2. D.G. Ravenhall, C.J. Pethick, and J.R. Wilson,*Phys. Rev. Lett.* **50** (1983) 2066.
3. M. Hashimoto, H. Seki, and M. Yamada, *Prog. Theor. Phys.* **71** (1984) 320.
4. C.J. Horowitz, M.A. Perez-Garcia, and J. Piekarewicz, *Phys. Rev. C* **69** (2004) 045804, astro-ph/0401079.
5. C.J. Horowitz, M.A. Perez-Garcia, J. Carriere, D.K. Berry, and J. Piekarewicz, *Phys. Rev. C* **70** (2004) 065806, astro-ph/0409296.
6. G.A. Lalazissis, J. Konig, and P. Ring, *Phys. Rev. C* 55 (1997)

540, nucl-th/9607039.

7. G.A. Lalazissis, S. Raman, and P. Ring, *At. Data Nucl. Data Tables* **71** (1999) 1.
8. J.D. Walecka, *Annals Phys.* **83** (1974) 491.
9. B.D. Serot and J.D. Walecka, *Adv. Nucl. Phys.* **16** (1986) 1.
10. B.D. Serot and J.D. Walecka, *Int. J. Mod. Phys. E* **6** (1997) 515, nucl-th/9701058.
11. B.G. Todd-Rutel and J. Piekarewicz, *Phys. Rev. Lett* **95** (2005) 122501, nucl-th/0504034.
12. H. Mueller and B.D. Serot, *Nucl. Phys. A* **606** (1996) 508, nucl-th/9603037.
13. C.J. Horowitz and J. Piekarewicz, *Phys. Rev. Lett.* **86** (2001) 5647, astro-ph/0010227.
14. C.J. Horowitz and B.D. Serot, *Nucl. Phys. A* **368** (1981) 503.
15. D.H. Youngblood, C.M. Rozsa, J.M. Moss, D.R. Brown, and J.D. Bronson, *Phys. Rev. Lett.* **39** (1977) 1188.
16. J. Boguta and A.R. Bodmer, *Nucl. Phys. A 292* (1977) 413.
17. C.J. Horowitz and J. Piekarewicz, *Phys. Rev. C 64* (2001) 062802, nucl-th/0108036.
18. C.J. Horowitz, S.J. Pollock, P.A. Souder, and R. Michaels, *Phys. Rev. C* **63** (2001) 025501, nucl-th/9912038.
19. R. Michaels, P.A. Souder, and G.M. Urciuoli (2005), URL http://hallaweb.jlab.org/ parity/prex
20. B.A. Brown, *Phys. Rev. Lett.* 85 (2000) 5296.
21. J. Carlson, S.-Y. Chang, V.R. Pandharipande, and K.E. Schmidt, *Phys. Rev. Lett.* **91** (2003) 050401.
22. G.A. Baker, *Phys. Rev. C* **60** (1999) 054311.
23. H. Heiselberg, *Phys. Rev. A 63* (2002) 043606 cond-mat/0002056.
24. Y. Nishida and D.T. Son, *Phys. Rev. Lett. 97* (2006) 050403 cond-mat/0604500.
25. A. Schwenk and C.J. Pethick, *Phys. Rev. Lett.* 95 (2005) 160401, nucl-th/0506042.
26. B. Friedman and V. R. Pandharipande, *Nucl. Phys. A 361* (1981) 502.
27. P. Danielewicz, R. Lacey, and W.G. Lynch, *Science* **298** 1592 (2002), nucl-th/0208016.
28. J. Cottam, F. Paerels, and M. Mendez, *Nature* **420** (2002) 51 astro-ph/0211126.
29. F. Ozel, *Nature* **441** (2006) 1115.
30. A.R. Villarreal and T.E. Strohmayer, *Astrophys. J.* **614** (2004) L121, astro-ph/0409384.
31. D.J. Nice *et al.*, *Astrophys. J.* **634** (2005) 1242 astro-ph/0508050.